Video Article

# *In Situ* SIMS and IR Spectroscopy of Well-defined Surfaces Prepared by Soft Landing of Mass-selected Ions

Grant E. Johnson[1], K. Don Dasitha Gunaratne[1], Julia Laskin[1]

[1]Physical Sciences Division, Pacific Northwest National Laboratory

Correspondence to: Julia Laskin at julia.laskin@pnnl.gov

URL: https://www.jove.com/video/51344
DOI: doi:10.3791/51344

Keywords: Chemistry, Issue 88, soft landing, mass selected ions, electrospray, secondary ion mass spectrometry, infrared spectroscopy, organometallic, catalysis

Date Published: 6/16/2014

Citation: Johnson, G.E., Gunaratne, K.D., Laskin, J. *In Situ* SIMS and IR Spectroscopy of Well-defined Surfaces Prepared by Soft Landing of Mass-selected Ions. *J. Vis. Exp.* (88), e51344, doi:10.3791/51344 (2014).

## Abstract

Soft landing of mass-selected ions onto surfaces is a powerful approach for the highly-controlled preparation of materials that are inaccessible using conventional synthesis techniques. Coupling soft landing with *in situ* characterization using secondary ion mass spectrometry (SIMS) and infrared reflection absorption spectroscopy (IRRAS) enables analysis of well-defined surfaces under clean vacuum conditions. The capabilities of three soft-landing instruments constructed in our laboratory are illustrated for the representative system of surface-bound organometallics prepared by soft landing of mass-selected ruthenium tris(bipyridine) dications, $[Ru(bpy)_3]^{2+}$ (bpy = bipyridine), onto carboxylic acid terminated self-assembled monolayer surfaces on gold (COOH-SAMs). *In situ* time-of-flight (TOF)-SIMS provides insight into the reactivity of the soft-landed ions. In addition, the kinetics of charge reduction, neutralization and desorption occurring on the COOH-SAM both during and after ion soft landing are studied using *in situ* Fourier transform ion cyclotron resonance (FT-ICR)-SIMS measurements. *In situ* IRRAS experiments provide insight into how the structure of organic ligands surrounding metal centers is perturbed through immobilization of organometallic ions on COOH-SAM surfaces by soft landing. Collectively, the three instruments provide complementary information about the chemical composition, reactivity and structure of well-defined species supported on surfaces.

## Video Link

The video component of this article can be found at https://www.jove.com/video/51344/

## Introduction

Soft landing of mass-selected ions onto surfaces remains a subject of current research interest due to the demonstrated capabilities of the technique for the highly-controlled preparation of novel materials[1-6]. Recent efforts have indicated potential future applications of soft landing of mass-selected ions in the preparation of peptide and protein arrays for use in high-throughput biological screening[7,8], separation of proteins and conformational enrichment of peptides[9-12], covalent attachment of peptides to surfaces[9,10,13,14], chiral enrichment of organic compounds[15], electrochemical characterization of specific redox-active proteins[16-18], production of thin molecular films[19,20], processing of macromolecules such as graphene[21] and preparation of model catalyst systems through soft landing of ionic clusters[22-39], nanoparticles[40-48] and organometallic complexes onto support materials[19,49-56]. The concept of modifying surfaces through soft landing of polyatomic ions was initially proposed by Cooks and co-workers in 1977[57]. In the subsequent years a wide range of instrumental approaches have been developed for the controlled deposition of mass-selected ions from the gas-phase onto surfaces[1,4,5]. Ions have been produced through processes such as electrospray ionization (ESI)[10,58,59], matrix- assisted laser desorption/ionization (MALDI)[21], electron impact ionization (EI)[60,61], pulsed arc discharge[62], inert gas condensation[36,63], magnetron sputtering[64,65], and laser vaporization[25,66,67]. Mass selection of gas-phase ions prior to soft landing has been achieved principally employing quadrupole mass filters[58,68,69], magnetic deflection devices[70], and linear ion trap instruments[8,59]. A particularly notable advance in ion soft landing methodology occurred recently with the successful implementation of ambient ion soft- and reactive landing by Cooks and co-workers[71,72]. Using these various ionization and mass-selection techniques, the interactions of hyperthermal (<100 eV) polyatomic ions with surfaces have been studied in order to better understand the factors influencing the efficiency of ion soft landing and the competing processes of reactive and unreactive scattering as well as surface induced dissociation[4,73-75].

The preparation of well-defined model catalysts for research purposes has been a particularly fruitful application of soft landing of mass-selected ions[25,34,35,56,76-81]. In the size range of nanoscale clusters, where physical and chemical behavior does not scale linearly with cluster size, it has been demonstrated that the addition or removal of single atoms to or from clusters may drastically influence their chemical reactivity[82-84]. This nanoscale phenomenon, which results from quantum confinement, was demonstrated convincingly by Heiz and co-workers[85] for a model catalyst consisting of soft landed clusters of eight gold atoms ($Au_8$) supported on a defect-rich MgO surface. Several additional studies have provided evidence of the size-dependent reactivity of clusters supported on surfaces[34,77,86,87]. Moreover, high resolution electron microscopy images indicate that clusters containing as few as ten[88] and fifty five[89] atoms may be largely responsible for the superior activity of bulk-synthesized gold catalysts supported on iron oxides. Employing soft landing of mass-selected ions, it is possible to prepare stable arrays of size-selected clusters and nanoparticles that do not diffuse and agglomerate into larger structures on the surface of support materials[90-92]. These previous studies indicate that with continuing development, soft landing of mass-selected clusters and nanoparticles may become a versatile technique for the

 

creation of highly active heterogeneous catalysts that exploit the emergent behavior of large numbers of identical clusters and nanoparticles in extended arrays on surfaces. These extremely well-defined systems may be used for research purposes to understand how critical parameters such as cluster size, morphology, elemental composition and surface coverage influence catalytic activity, selectivity and durability.

Organometallic complexes that are typically used in the solution-phase as homogeneous catalysts also may be immobilized on surfaces through soft landing of mass-selected ions[56,80,81]. Attaching ionic metal-ligand complexes to solid supports to produce hybrid organic-inorganic materials is currently an active area of research in the catalysis and surface science communities[93]. The overall goal is to obtain the high selectivity toward a desired product of solution-phase metal-ligand complexes while facilitating an easier separation of products from catalysts and reactants remaining in solution. In this manner, surface immobilized organometallic complexes reap the benefits of both homogeneous and heterogeneous catalysts. Through selection of an appropriate substrate it is possible to maintain or even enhance the organic ligand environment around the active metal center while also achieving strong surface immobilization[94]. Self-assembled monolayer surfaces (SAMs) on gold may be terminated with a number of different functional groups and are, therefore, ideal systems to investigate the feasibility of tethering organometallic complexes to surfaces through soft landing of mass-selected ions[95]. Furthermore, ionization methods such as atmospheric pressure thermal desorption ionization (APTDI) have been demonstrated previously to yield gas-phase mixed-metal inorganic complexes that are not accessible through synthesis in solution[96]. In a similar vein, non-thermal kinetically-limited synthesis and ionization techniques such as magnetron sputtering[65], gas aggregation[63] and laser vaporization[66] also may be coupled with ion soft landing instrumentation to provide a versatile route to novel inorganic clusters and nanoparticles supported on surfaces.

In order to evolve soft landing of mass-selected ions into a mature technology for the preparation of materials, it is critical that informative analytical methods be coupled with soft landing instrumentation to probe the chemical and physical properties of surfaces before, during and after deposition of ions. To date, a multitude of techniques have been applied for this purpose including secondary ion mass spectrometry (SIMS)[19,97-100], temperature programmed desorption and reaction[50,52], laser desorption and ionization[101], pulsed molecular beam reaction[102], infrared spectroscopy (FTIR and Raman)[98,103,104], surface enhanced Raman spectroscopy[103,105], cavity ringdown spectroscopy[106], x-ray photoelectron spectroscopy[35,107], scanning tunneling microscopy[33,108-111], atomic force microscopy[112-114], and transmission electron microscopy[39]. However, to most accurately characterize surfaces prepared or modified by ion soft landing, it is crucial that the analysis be performed *in situ* without exposure of the substrate to the environment in the laboratory. Previous analyses conducted *in situ* have provided insight into phenomena such as the reduction of ionic charge of soft landed ions over time[37,38,115,116], the desorption of soft landed ions from surfaces[52], the efficiency and kinetic energy dependence of ion reactive landing[14,81], and the influence of size on the catalytic activity of clusters and nanoparticles deposited onto surfaces[117]. By way of example, in our laboratory, we have systematically studied the charge reduction kinetics of protonated peptides on the surfaces of different SAMs[3]. These experiments were performed with a unique soft landing instrument coupled to a Fourier transform ion cyclotron resonance secondary ion mass spectrometer (FT-ICR-SIMS) that enables *in situ* analysis of surfaces both during and after soft landing of ions[97]. To expand upon these analytical capabilities, another instrument was constructed that allows *in situ* characterization of soft landed ions on surfaces using IRRAS[104]. This surface-sensitive infrared technique enables bond formation and destruction processes as well as conformational changes in complex ions and surface layers to be monitored in real time both during and after soft landing[12]. For instance, using IRRAS it was demonstrated that ion soft landing may be used to covalently immobilize mass-selected peptides on *N*-hydroxysuccinimidyl ester functionalized SAMs[13,14].

Herein, we illustrate the capabilities of three unique custom-built instruments located at the Pacific Northwest National Laboratory that are designed for *in situ* TOF-SIMS, FT-ICR-SIMS, and IRRAS analysis of substrates produced through soft landing of mass-selected ions onto surfaces. As a representative system, we present results for soft landing of mass-selected organometallic ruthenium tris(bipyridine) dications $[Ru(bpy)_3]^{2+}$ onto carboxylic acid terminated SAMs (COOH-SAMs) to prepare immobilized organometallic complexes. It is shown that *in situ* TOF-SIMS offers the advantages of extremely high sensitivity and large overall dynamic range which facilitates identification of low abundance species including reactive intermediates that may only be present for short periods of time on the surfaces. TOF-SIMS also provides insight into how the removal of a ligand from an organometallic ion in the gas-phase, prior to soft landing, influences its efficiency toward immobilization on surfaces and its chemical reactivity towards gaseous molecules. Complementary characterization using *in situ* FT-ICR-SIMS provides insights into the charge reduction, neutralization and desorption kinetics of the doubly charged ions on the surface while *in situ* IRRAS probes the structure of the organic ligands surrounding the charged metal centers, which may influence the electronic properties and reactivity of the immobilized ions. Collectively, we illustrate how soft landing of mass-selected ions combined with *in situ* analysis by SIMS and IRRAS provides insight into the interactions between well-defined species and surfaces which have implications for a broad range of scientific endeavors.

## Protocol

# 1. Preparation of COOH-SAM Surfaces on Gold for Soft Landing of Mass-selected Ions

1. Obtain flat gold substrates on silicon (Si) or mica backing materials. Alternatively, prepare gold films on Si or mica surfaces according to procedures described in the literature[118,119]. Note: Use surfaces that have the following specifications: 1 $cm^2$ or circular and 5 mm in diameter, 525 µm thick Si layer, 50 Å thick Ti adhesion layer, 1,000 Å Au layer.
2. Place fresh gold-on-silicon surfaces into glass scintillation vials and immerse in pure (non-denatured) ethanol.
3. Place scintillation vials containing gold surfaces immersed in ethanol into an ultrasonic cleaner and wash for 20 min to remove any surface debris. Note: Do not ultrasonically wash gold on mica surfaces as this will detach the gold film from the mica backing material.
4. Remove washed gold surfaces from vials and dry with a stream of pure $N_2$ to prevent the formation of any residual spots from the ethanol.
5. Place the dried gold surfaces face up in an ultraviolet (UV) cleaner and irradiate for 20 min to remove surface organic matter.
6. In glass scintillation vials, prepare 5 ml of 1 mM solutions of 16-mercaptohexadecanoic acid (COOH-SAM) in non-denatured ethanol.
7. Add hydrochloric acid to a final concentration of 1% HCl in ethanol to ensure protonation of the carboxylic acid groups of the molecules.
8. Place the washed, dried and UV-cleaned gold surfaces face up into the COOH-SAM solutions ensuring that the entire gold surface is fully immersed in each vial. Allow the monolayer surfaces on gold to assemble for at least 24 hr in the dark (wrap vials in foil).
9. Remove the surfaces from the COOH-SAM solutions and place in new scintillation vials containing 5 ml of 1% HCl in ethanol. Ultrasonically wash the SAM surfaces for 5 min to remove any physisorbed molecules from the monolayer surface.

10. Remove the washed surfaces from the vials and rinse with several 1 ml aliquots of 1% HCl in ethanol. Dry the COOH-SAM surfaces under a stream of $N_2$.
11. Using clean metal forceps and wearing gloves place a SAM surface onto one of three metal sample mounts that are compatible with each soft landing instrument taking care not to touch the front facing gold surface in the process. Ensure that the surface is fixed tightly in place and that there is strong electrical contact between the back side of the surface and the metal sample mount.
12. Employing the load-lock sample introduction capabilities of the soft landing instruments (each is slightly different), ensure that the gate valve separating the sample introduction region of the instrument from the soft landing chamber is closed. Bring the sample introduction chamber up to atmospheric pressure by turning off the turbomolecular vacuum pump and ionization pressure gauge and closing the valve to the foreline mechanical vacuum pump.
13. When the sample introduction chamber reaches atmospheric pressure open the sample door and secure the sample holder firmly to the manipulator (xyz-stage or z-translator) inside of the instrument. Close the door and open the valve to the foreline mechanical vacuum pump. When the sample introduction chamber reaches a pressure of $10^{-3}$ Torr, turn on the turbomolecular vacuum pump and ionization pressure gauge.
14. When the sample introduction chamber reaches a pressure of $10^{-5}$ Torr, open the gate valve to the soft landing chamber. Use the magnetic manipulator or xyz-stage to position the SAM surface in line with the ion beam to begin soft landing.

## 2. Soft Landing of Mass-selected $Ru(bpy)_3^{2+}$ onto COOH-SAM Surfaces

1. Obtain tris(2,2'-bipyridyl)dichloro-ruthenium(II) hexahydrate solid. Dissolve the red crystals in pure methanol to create stock solutions with a concentration of $10^{-3}$ M. Dilute the stock solutions by a factor of either 10 or 100 with methanol to achieve optimum electrospray ion current of mass-selected $Ru(bpy)_3^{2+}$ *m/z* = 285.
2. Load the diluted solutions into 1 ml glass syringes. Use a syringe pump to infuse the solution through a 360 µm outer diameter 80 µm inner diameter fused silica capillary that is biased between +2 to +3 kV to generate positive ions. Adjust the syringe pump flow rate between 20-40 µl/hr to obtain optimum ion current and stability at the surface.
3. Adjust the quadrupole mass-filter to the mass of the $Ru(bpy)_3^{2+}$ ion *m/z* = 285 to prevent soft landing of species other than $Ru(bpy)_3^{2+}$ onto the surface. Using a high-resistance electrometer connected to the substrate through a vacuum electrical feed-through, adjust the voltage settings of the ion optics and radiofrequency ion guides to maximize the ion current and stability of $Ru(bpy)_3^{2+}$ measured at the SAM surface. Allow the experiment to run for a selected period of time to achieve the desired coverage of ions on the surface of the COOH-SAM.
4. Increase the potential gradient in the high-pressure collision quadrupole region of the soft landing instruments to create the harsh conditions that enable gas-phase ligand stripping from the organometallic ion through collision induced dissociation. Note: Examine the schematic diagram of one of the three soft landing instruments, which is also representative of the early stages of the other two instruments, which is presented in **Figure 1**. The fragmentation of the $Ru(bpy)_3^{2+}$ ion occurs in region 4. Increase the voltage applied to the back plate of the electrodynamic ion funnel to remove one bipyridine ligand from $Ru(bpy)_3^{2+}$ *m/z* = 285 producing gas-phase $Ru(bpy)_2^{2+}$ *m/z* = 207 in region 4 of the instrument[81]. Mass select the highly reactive undercoordinated fragment ion using the quadrupole mass filter in region 6 of the instrument and soft land onto COOH-SAM surfaces to examine how the extent of ligation influences the properties of supported organometallic ions.
5. Adjust the surrounding ion optics, including the DC voltages applied to the quadrupole rods as well as the conductance limit to maximize the current of mass-selected $Ru(bpy)_2^{2+}$ fragment ions at the surface.

## 3. Analysis by *In Situ* TOF-SIMS Before and After Exposure to Reactive Gases

1. Turn off the syringe pump and high voltage to the ESI emitter. Open the gate valve that separates the two regions of the instrument during operation. Use the magnetic manipulator to move the prepared surface from the soft landing chamber to the analysis stage inside the TOF-SIMS part of the instrument.
2. Disengage the manipulator from the sample and retract it fully from the SIMS analysis chamber. Close the gate valve between the soft landing and SIMS parts of the instrument because the TOF-SIMS operates at a much lower pressure than the soft landing region of the instrument.
3. To conduct the TOF-SIMS experiment, load the instrument control file in the software and ensure that the $Ga^+$ source is producing a sufficiently stable current of primary ions. Note: Employ 15 keV primary gallium ions ($Ga^+$, 500 pA, 5 nsec pulse width, 10 kHz repetition rate) to induce desorption of soft landed material from the surfaces. Extract secondary ions ejected from the surface into the mass analyzer, which consists of three separate electrostatic sectors.
4. Acquire x- and y-axis line profiles across the surface to determine the center of the deposited spot of ions on the substrate (typically at the center of the surface and 3 mm in diameter). Position the surface so that the $Ga^+$ primary ion beam is incident on the center of the deposited spot of ions. Acquire a TOF-SIMS mass spectrum for 5 min.
5. Turn off the primary $Ga^+$ ion beam and high voltages of the TOF-SIMS. Use the magnetic manipulator to move the sample back into the soft landing part of the instrument. Make sure that the gate valve separating the two chambers is closed before proceeding further.
6. Use a high-vacuum leak valve on the soft landing chamber to introduce a controlled flow of ultra-high purity oxygen ($O_2$) gas from a cylinder into the instrument. Use the adjustable gate valve in front of the turbomolecular vacuum pump to throttle the pumping speed of the pump to achieve a steady-state pressure of $10^{-4}$ Torr of $O_2$ inside the soft landing chamber.
7. Following exposure of the surface to $O_2$ for 30 min close the leak valve, open the gate valve over the turbomolecular vacuum pump and allow the remaining $O_2$ to pump away. After the pressure in the chamber has decreased, open the gate valve to the SIMS part of the instrument and use the magnetic manipulator to position the surface on the analysis platform for a second round of TOF-SIMS analysis.
8. After the second TOF-SIMS spectrum is obtained as described in sections 3.3-3.4, open the gate valve and position the surface back in the soft landing chamber for exposure to $10^{-4}$ Torr of $C_2H_4$ for 30 min. Perform a SIMS analysis again as described above.

## 4. Analysis by *In Situ* FT-ICR-SIMS During and After Soft Landing

1. Prepare the SAM surfaces for experiments with the *in situ* FT-ICR-SIMS instrument in a manner similar to that described in section 1 but on circular substrates 5 mm in diameter. Note: Use substrates that are laser cut from a gold coated silicon wafer (5 nm chromium adhesion layer and 100 nm of polycrystalline vapor-deposited gold). Be aware that the most notable difference is that in the FT-ICR-SIMS instrument the surface is positioned inside the bore of a superconducting magnet. The presence of the magnet necessitates that the surfaces be placed at the end of a 5 ft manual z-translator to enable them to be positioned safely and adjustably at the rear plate of the ICR cell.
2. Using the load-lock interface, position a circular SAM surface at the rear trapping plate of the ICR cell located inside of the 6 Tesla magnet. Note: Be aware that this instrument is a specially designed 6-Tesla FT-ICR mass spectrometer configured for studying ion-surface interactions[97,120].
3. Operate the ion soft landing portion of the FT-ICR-SIMS instrument in a manner similar to that described in section 2.
4. Use a cesium ion source to create a continuous beam of 8 kV $Cs^+$ primary ions to sputter the surface during and after ion soft landing.
5. Utilize the ESI source positioned at 90° toward the main instrument axis to generate ions for soft landing. Focus the ions through a 90° bending quadrupole[120]. Note: Be aware this instrument geometry facilitates simultaneous soft landing of $Ru(bpy)_3^{2+}$ and transmission of the primary $Cs^+$ ion beam to the surface thereby enabling the monitoring of the soft landing process both during and after ion deposition.
6. Trap and analyze the secondary ions ejected from the surface using FT-ICR-MS. Note: Employ static SIMS conditions corresponding to a total ion flux of about $10^{10}$ ions/$cm^2$ (current 4 nA, duration 80 µsec, spot diameter 4.6 mm, 10 shots per spectrum, ~200 data points) for these experiments that last for about 7 hr. Average each SIMS spectrum over 10 shots corresponding to an acquisition time of ~10 sec.
7. Acquire kinetics data by sampling the SAM surface every 4 min for approximately 7 hr during and after ion deposition.
8. Perform data acquisition and instrument control using an automated modular data control system described in the literature[121].

## 5. Analysis by *In Situ* IRRAS During and After Soft Landing

1. Prepare the SAM surfaces for experiments with the *in situ* IRRAS instrument in a manner similar to that described in section 1. Note: Be aware that the largest difference with the IRRAS instrument results from the precise positioning of the surface with the z-translator that is necessary to locate the substrate at the focal point of the parabolic mirrors and in line with the beam of ions. Maximize the overlap between the infrared beam and the spot of deposited ions on the surface.
2. Conduct the IRRAS experiments in a grazing-incidence geometry employing an FTIR spectrometer equipped with a liquid nitrogen cooled mercury-cadmium-telluride (MCT) detector.
3. Utilize a gold-coated flat mirror to direct the light exiting the FTIR spectrometer onto a parabolic gold mirror. Reflect the light from the parabolic mirror through a mid-infrared wire grid polarizer and into the vacuum chamber through a viewport.
4. Direct the infrared light from the spectrometer onto the COOH-SAM surface positioned inside the vacuum chamber. Note: The vacuum chamber is held at a pressure of $10^{-5}$ Torr during ion soft landing.
5. Position the reflective SAM on gold surface inside the vacuum chamber at the focal point of the first parabolic mirror using the motor-driven z-translator.
6. Reflect the IR light entering the vacuum chamber from the surface of the SAM and out of the chamber through a second viewport. Use a second parabolic gold mirror to focus the reflected light from the surface onto an MCT detector.
7. Purge the pathway of the IR beam outside of the vacuum chamber with $N_2$.
8. Acquire spectra at set intervals during the deposition.

# Representative Results

## 1. Investigating the Reactivity of $Ru(bpy)_3^{2+}$ on COOH-SAMs Using *In Situ* TOF-SIMS

Soft landing of mass-selected organometallic ions onto functionalized SAMs is first illustrated using *in situ* TOF-SIMS to provide maximum sensitivity toward detection of adducts formed between the deposited ions and the individual molecules in the monolayers as well as any products of chemical reactions following exposure of the surfaces to reactive gases. The doubly charged $Ru(bpy)_3^{2+}$ ion originates from dissolution and dissociation of solid-phase tris(2,2'-bipyridyl)dichlororuthenium(II) hexahydrate crystals in methanol. The $Ru(bpy)_3^{2+}$ *m/z* = 285 dication selected for the representative soft landing experiments described herein is the most abundant ion generated from electrospray ionization of the solution. Undercoordinated $Ru(bpy)_2^{2+}$ ions are prepared by fragmentation of one bipyridine ligand from each fully ligated $Ru(bpy)_3^{2+}$ ion. This is induced by gas-phase collision-induced-dissociation in the first quadrupole region of the soft landing instrument shown schematically in **Figure 1**. An ion current of around 100 pA and 60 pA is directed at the COOH-SAM surfaces for 30 and 45 min for $Ru(bpy)_3^{2+}$ and $Ru(bpy)_2^{2+}$, respectively, corresponding to a total delivery of 5 x $10^{11}$ mass-selected ions to a circular spot approximately 3 mm in diameter. The kinetic energy of the ions approaching the surface is determined by adjusting the potentials applied to the second collision quadrupole (see **Figure 1**) and the surface. The kinetic energy is set at around 10 eV per charge for all of the soft landing experiments conducted using the *in situ* TOF-SIMS apparatus.

Following soft landing of 5 x $10^{11}$ intact $Ru(bpy)_3^{2+}$ ions onto the surface of the COOH-SAM, a number of new peaks that are not present prior to deposition become prominent in the TOF-SIMS spectra. Isotopic envelopes corresponding to intact doubly charged $Ru(bpy)_3^{2+}$ *m/z* = 285 and singly charged $Ru(bpy)_3^+$ *m/z* = 570 are observed following soft landing of $Ru(bpy)_3^{2+}$ onto the COOH-SAM surface. The relative abundance of these species suggests that reduction of the ionic charge of $Ru(bpy)_3^{2+}$ to $Ru(bpy)_3^+$ takes place rapidly on the surface of the COOH-SAM. Another isotopic envelope is present at *m/z* = 414 which corresponds to the fragment $Ru(bpy)_2^+$. This singly charged ion, which results from loss of one bipyridine ligand from singly charged $Ru(bpy)_3^+$, is likely formed through dissociation of $Ru(bpy)_3^+$ during analysis by TOF-SIMS. In contrast, the TOF-SIMS spectrum obtained following soft landing of the fragment $Ru(bpy)_2^{2+}$ lacks any of the characteristic peaks related to the intact complex (*i.e.* $Ru(bpy)_3^{2+}$ or $Ru(bpy)_3^+$). Most importantly, a peak corresponding to a $Ru(bpy)_2$-thiol$^+$ adduct at *m/z* = 700 is observed

which indicates very strong binding between the undercoordinated ion and the monolayer surface. The peaks corresponding to this species are featured prominently in **Figure 2a**.

After soft landing, the COOH-SAM surfaces are exposed to controlled pressures of either $O_2$ or $C_2H_4$ in the deposition region of the instrument to examine the chemical reactivity of the immobilized organometallic complexes. Following gas exposure, the surfaces are analyzed again by *in situ* TOF-SIMS. Presented in **Figures 2b** and **2c** are the *in situ* TOF-SIMS spectra obtained directly following exposure of the COOH-SAM surfaces containing soft landed $Ru(bpy)_3^{2+}$ and $Ru(bpy)_2^{2+}$ ions to $O_2$ and $C_2H_4$. As discussed in the preceding paragraph, following soft landing of $Ru(bpy)_{2/3}^{2+}$ onto COOH-SAM surfaces an isotopic distribution corresponding to an electrostatic adduct formed between the ions and the surface molecules is observed. After exposure of the surface to $10^{-4}$ Torr of $O_2$ for 30 min the TOF-SIMS spectra indicate that there is an obvious reduction in the abundance of the adduct peak at *m/z* = 700 accompanied by a concomitant increase in the abundance of two new isotopic envelopes centered at *m/z* = 716.2 and 732.2. These peaks are consistent with the addition of atomic (O) and molecular ($O_2$) oxygen to the organometallic surface adduct, respectively. Moreover, this adduct appears to be oxidized with close to 50% conversion efficiency. After exposure to $O_2$ and analysis by *in situ* TOF-SIMS the surfaces are positioned back into the soft landing region of the instrument and exposed to $10^{-4}$ Torr of $C_2H_4$ for 30 min. Following the second gas exposure the surface is transferred again to the SIMS region of the instrument for another round of analysis. Inspection of the TOF-SIMS spectrum following exposure to $C_2H_4$ indicates a decrease in the relative abundance of the singly oxidized organometallic adduct at *m/z* = 716. This observation is consistent with deoxygenation of the immobilized organometallic complex upon exposure to $C_2H_4$. This is hypothesized to result in the formation of the oxidized hydrocarbon ($C_2H_4O$), which is released to the gas-phase. Therefore, through a combination of soft landing of mass selected ions and analysis by *in-situ* TOF-SIMS it is possible to selectively isolate organometallic compounds on surfaces and examine their reactivity towards gaseous molecules. In addition, the behavior of undercoordinated ions that are not accessible in solution may be examined. A scheme describing what is achieved for this representative system through the combination of ion soft landing and analysis by *in-situ* TOF-SIMS is presented in **Figure 3**.

## 2. Studying the Charge Retention of $Ru(bpy)_3^{2+}$ on COOH-SAMs Using *In Situ* FT-ICR-SIMS

Soft-landing of mass-selected ions is also conducted employing a second instrument that enables analysis of the surfaces by *in situ* FT-ICR-SIMS. This complementary approach, which enables SIMS analysis of the surfaces both during and after soft landing of ions, is capable of providing insight into the kinetics of charge reduction and neutralization as well as the desorption of ions deposited on surfaces[115]. It is a particularly powerful technique because the relative abundance of different ionic charge states on the surface may be monitored over periods of several hours. Representative results for $Ru(bpy)_3^{2+}$ soft landed onto a COOH-SAM surface are presented in **Figure 4**. During soft landing the doubly charged $Ru(bpy)_3^{2+}$ ion exhibits a linear increase in abundance on the COOH-SAM surface. The measured abundance reaches a maximum at the end of soft landing and is followed by an extended plateau on the COOH-SAM surface. This indicates that the COOH-SAM surface is particularly effective at preserving the ionic charge state of the intact ions following soft landing. The singly charged $Ru(bpy)_3^{+}$ ion also exhibits a linear increase in abundance with respect to time during soft landing. At the end of soft landing, however, the singly charged ion decreases in abundance. The abundance of the singly charged fragment ion resulting from loss of one bipyridine ligand from $Ru(bpy)_3^{+}$ forming $Ru(bpy)_2^{+}$ is also shown in **Figure 4**. This ion displays a linear increase in abundance during soft landing followed by a decline in abundance on the COOH-SAM after the end of deposition. Because the binding energy of ions to the surface increases with the charge state, it is reasonable to assume that singly charged ions undergo more facile desorption from the surface as compared to the doubly charged ions, which is consistent with the faster loss of singly charged ions observed in this study. Soft landing coupled with *in situ* FT-ICR-SIMS is, therefore, a powerful technique for investigating processes such as the reduction of charge, neutralization and desorption of ions deposited on surfaces.

## 3. Probing the Structural Features of $Ru(bpy)_3^{2+}$ on COOH-SAMs Employing *In Situ* IRRAS

The third instrument used for characterizing soft-landed ions is able to obtain vibrational spectra of the $Ru(bpy)_3^{2+}$ ions on the COOH-SAMs in addition to detecting changes to the chemically-modified surface due to ion-surface interactions. This instrument is particularly powerful because it measures changes in the vibrational features of the surface both during and after soft landing. Therefore, a wealth of structural information regarding soft landed ions may be obtained using this instrument, provided that sub-monolayer levels of ions are deposited and that the transition dipole moments of the soft landed ions are aligned favorably and possess sufficient intensity to interact with the polarized IR photons incident on the surface.

The infrared spectrum obtained following soft landing of $5 \times 10^{12}$ $Ru(bpy)_3^{2+}$ ions onto the COOH-SAM surface is presented in **Figure 5**. We note that because the IR spectrum of the bare COOH-SAM was used as the background spectrum, the features observed following ion deposition originate solely from the vibrational modes of the soft-landed ions. Nine vibrational features are noted with an asterisk in the IR spectrum as unique spectroscopic signatures of $Ru(bpy)_3^{2+}$. These IR features are in good agreement with previously assigned values for this organometallic ion[122,123]. Out of the observed vibrational frequencies, the C-C stretching (1,606; 1,570; 1,042 $cm^{-1}$) and C-C-H bending (1,466; 1,450; 1,420; 1,257; 1,186 $cm^{-1}$) bands as well as the IR signature of a C-N stretch at 1,549 $cm^{-1}$ are assigned as unique features of the molecular structure of $Ru(bpy)_3^{2+}$. When conducting ion soft landing experiments, it is desirable to characterize the surface using spectroscopy techniques in order to confirm the identity of the species deposited and to gain insights into possible changes in structure that may result from ion-surface interactions. To this end, the *in situ* IRRAS soft landing instrument proves to be a valuable resource that contributes to the broader information gathered about the system of interest using TOF and FT-ICR-SIMS.

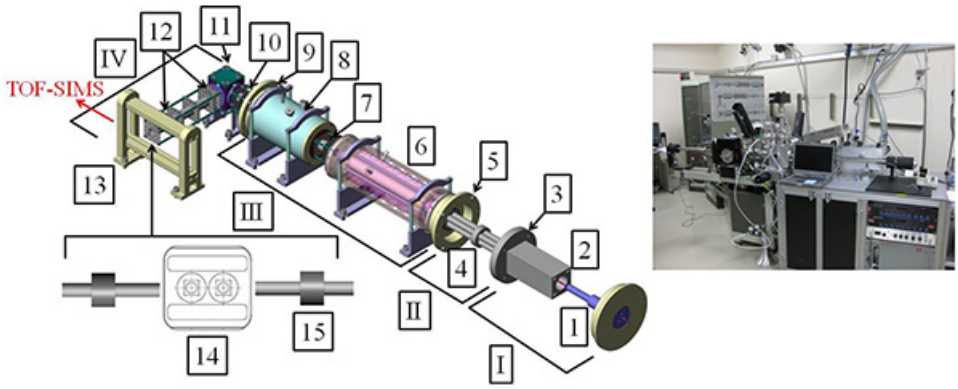


**Figure 1. Schematic illustration of the ion deposition instrument coupled to the TOF-SIMS:** I, ion funnel region (7 x $10^{-1}$ Torr). II, collision quadrupole region (1 x $10^{-1}$ Torr). III, mass selection and focusing region (2 x $10^{-4}$ Torr). IV, deposition region (1 x $10^{-6}$ Torr). (1) heated capillary, (2) electrodynamic ion funnel, (3) first conductance limit, (4) first collision quadrupole, (5) second conductance limit, (6) resolving quadrupole, (7) 2 focusing lenses, (8) second collision quadrupole, (9) third conductance limit, (10) Einzel lens, (11) quadrupole bender, (12) two Einzel lenses, (13) target platform, (14) surface mount, (15) magnetic translators. This figure has been modified from [*Analytical Chemistry* 2010, **82**(13), 5718-5727]. Click here to view larger image.

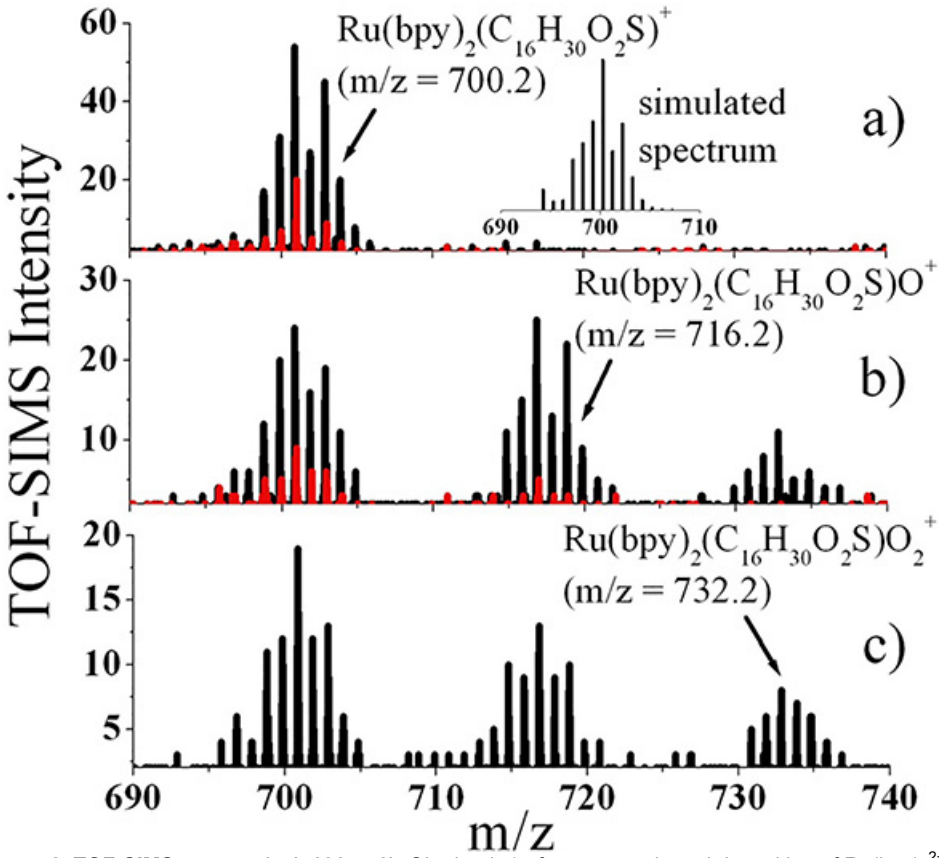


**Figure 2. TOF-SIMS spectra (*m/z* 690-740).** Obtained **a**) after mass-selected deposition of $Ru(bpy)_2^{2+}$ (black) and $Ru(bpy)_3^{2+}$ (red) onto the surface of COOH-SAM, **b**) after exposure to $O_2$ and **c**) after exposure to $C_2H_4$. This figure has been modified from [*Chemistry-A European Journal* 2010, **16**(48), 14433-14438]. Click here to view larger image.

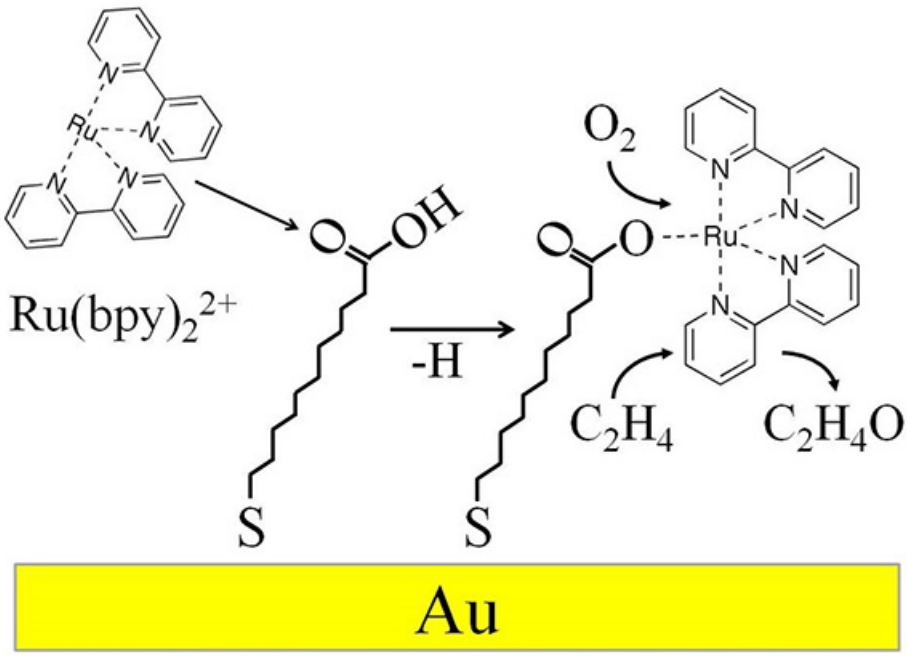


**Figure 3. Schematic representation of the immobilization of $Ru(bpy)_2^{2+}$ on COOH-SAM surfaces through gas-phase ligand stripping and soft landing of mass-selected ions.** This figure has been modified from [*Chemistry-A European Journal* 2010, **16**(48), 14433-14438]. Click here to view larger image.

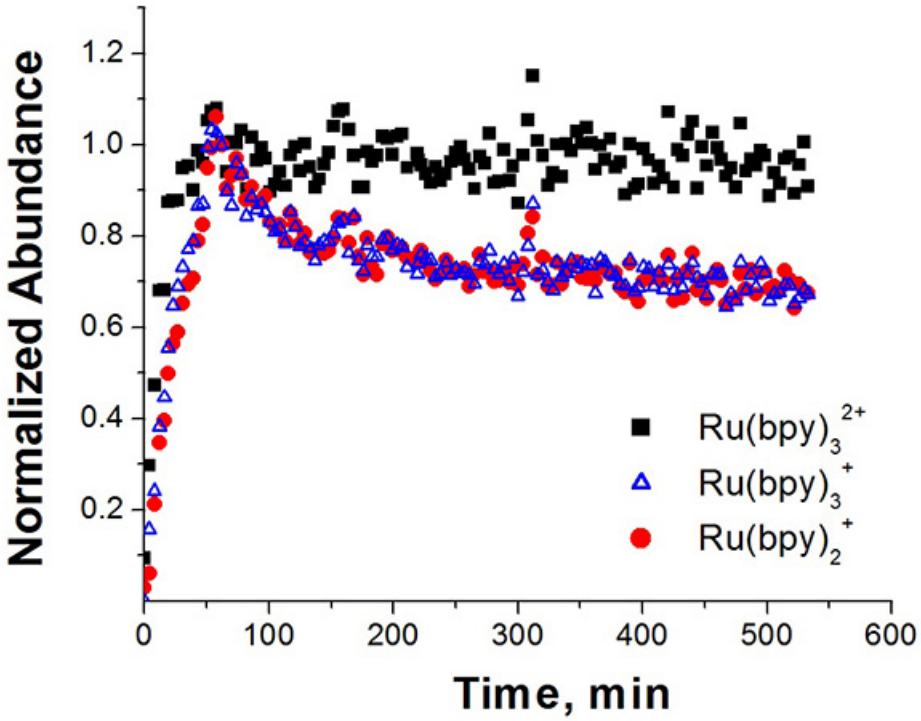


**Figure 4. FT-ICR SIMS kinetic plots.** Obtained for $Ru(bpy)_3^{2+}$ (*m/z* = 285, black squares), $Ru(bpy)_3^{+}$ (*m/z* = 570, blue triangles) and $Ru(bpy)_2^{+}$ (*m/z* = 414, red dots) following soft landing of $Ru(bpy)_3^{2+}$ onto a COOH-SAM surface. Click here to view larger image.

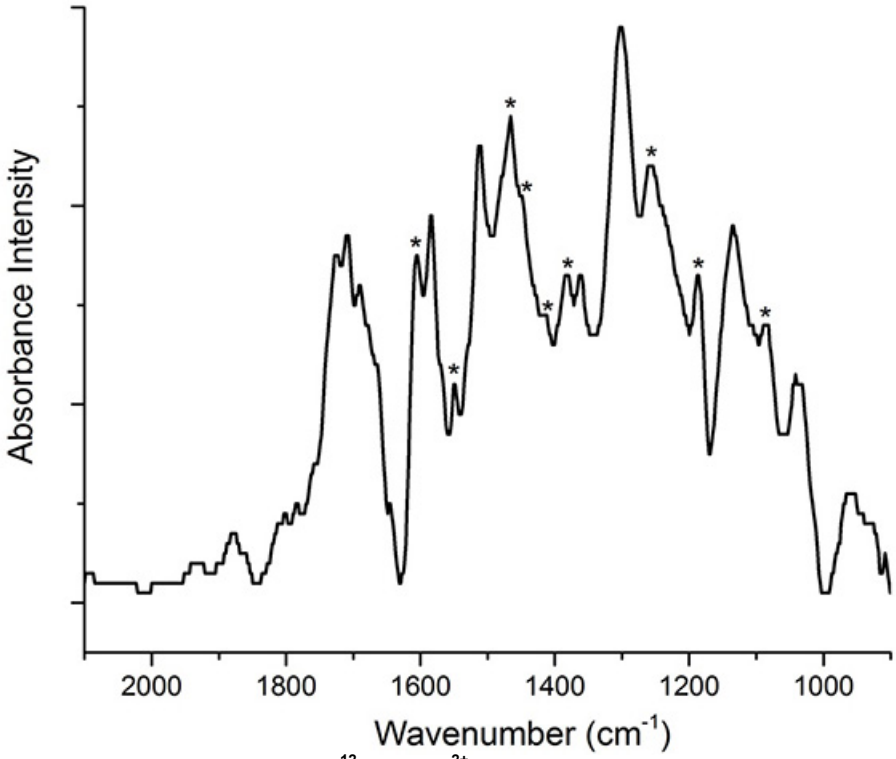


**Figure 5. IRRAS spectrum of ~5 x $10^{12}$ $Ru(bpy)_3^{2+}$ ions soft landed on the surface of a COOH-SAM.** The major vibrational features assigned to $Ru(bpy)_3^{2+}$ are denoted by an asterisk. Click here to view larger image.

## Discussion

Soft landing of mass-selected ions is generally conducted employing unique custom-built instrumentation that exists in several laboratories around the world that are specially equipped for these experiments. Modifications are constantly being made to these instruments to facilitate the ionization of a wider array of compounds, to achieve larger ion currents and shorter deposition times, to multiplex soft landing and thereby achieve simultaneous deposition of several species at different locations on the surface, and to allow more accurate selection of ions by both mass-to-charge ratio and ion mobility prior to deposition. In a similar fashion, a constantly changing lineup of characterization techniques is being coupled with ion soft landing instrumentation to enable *in situ* analysis of deposited material. Despite these differences between individual instruments, one of the most common problems encountered in soft landing experiments is the inability to route a sufficiently strong and stable beam of mass-selected ions from the source region of the instrument to the surface. This may result from poor ionization efficiency at the source, improperly adjusted voltages that steer the ions through the instrument, and poor electrical contact between the surface and the electrometer used to measure the current of soft landed ions. In such troublesome situations, the ion beam may be routed through the instrument manually by first maximizing the ion current measured at the earliest stage of the instrument and then systematically optimizing the current measured on each subsequent optic along the total beam path. Common problems encountered during *in situ* analysis of soft landed materials include large background signals from contaminant molecules such as adventitious hydrocarbons. For this reason it is critical that the surfaces are prepared carefully and reproducibly prior to each soft landing experiment.

Soft landing of mass-selected ions may be used to prepare extremely well-defined surfaces for subsequent analysis by *in situ* SIMS and IRRAS spectroscopy as well as a whole host of additional *ex situ* microscopy and spectroscopy techniques[6]. Mass selection offers precise control over the molecular composition and ionic charge state of soft landed materials. Furthermore, unprecedented surface cleanliness is obtainable with ion soft landing because common contaminants such as neutral molecules, counterions and solvent that are present in solution are removed from the ion beam prior to deposition so that only the mass-selected ions are delivered to the substrate under sterile vacuum conditions. The coverage of ions on the surface may be carefully controlled by monitoring the current of soft landed ions and varying the length of the deposition accordingly. The kinetic energy of the ions may be reduced to achieve soft landing conditions or increased to promote reactive landing through covalent bond formation[14] or “pinning” of ions into the surface[22].

*In situ* TOF-SIMS, compared to the other FT-ICR-SIMS technique, is generally characterized by greater sensitivity, larger dynamic range, less fragmentation of sputtered secondary ions, and fewer reactions of sputtered material in the plume of secondary ions. The larger dynamic range and higher sensitivity of TOF-SIMS enable detection of low-abundance species produced by ion soft landing onto surfaces. Using *in situ* TOF-SIMS it is possible to identify adducts that are formed between soft landed ions and individual molecules on monolayer surfaces. In addition, *in situ* TOF-SIMS illustrates that undercoordinated ions prepared by gas-phase collision induced dissociation may be more active towards surface immobilization than fully ligated ions. It should be noted that these undercoordinated metal ions do not exist in the solution phase and, therefore, represent novel species prepared using the capabilities of the soft landing instrumentation and identified using TOF-SIMS. Another powerful capability of the *in situ* TOF-SIMS instrument is the ability to expose the surfaces to controlled pressures of reactive gases and subsequently analyze any changes in surface composition without breaking vacuum.

*In situ* FT-ICR-SIMS, while generally less sensitive and prone to somewhat higher yields of fragment ions and products of gas-phase ion-molecule reactions than TOF-SIMS, offers the additional capability of being able to monitor the composition of the surface both during and after soft landing over a period of several hours. This information is critical to understanding processes such as reduction of charge and desorption of ions from the surface. For example, this instrument has been used previously to monitor redox chemistry taking place between two different ions soft landed onto the same SAMs[80]. In addition, the charge reduction and desorption kinetics of multiply protonated peptide ions also have been studied using this instrument and the data was applied to produce a kinetic model describing the evolution of different charged species on the surfaces of SAMs over time.

Employing *in situ* IRRAS, structural information about soft landed ions on surfaces may be obtained to verify that the ions retain their integrity during the deposition process. This is achieved by comparing the measured infrared spectra of ions on surfaces with previous spectra obtained by infrared spectroscopy in the gas phase and solution phase as well as IR spectra calculated using theoretical modeling. By comparing this known structural information with the measured vibrational features of the deposited samples, changes to the gas-phase structures may be identified. In addition, insight into ion-surface interactions may be ascertained from the observation of vibrational features that increase in intensity during the course of soft landing. Such an observation is consistent with the formation of new bonds at the surface. In a similar vein, vibrational features that decrease during the soft landing process may be indicative of bond-breaking reactions.

The controlled preparation of high-purity thin films on surfaces is necessary for a variety of applications in materials science and microfabrication[124]. Currently, a popular method for the preparation of thin organic films and hybrid organic-inorganic interfaces is molecular layer deposition (MLD) which depends on self-limiting interfacial reactions occurring between molecules and surfaces[125,126]. MLD enables a great deal of control over the deposition process and, therefore, generally produces higher-quality films on surfaces than solution-phase methods[127]. Nevertheless, despite the widespread commercial use of MLD, this technique is known to suffer from several key limitations which have been reviewed in a recent publication[128]. Most importantly, due to the fact that MLD relies on deposition of neutral molecules from the gas phase it is limited to thermally stable reactants that have enough vapor pressure to yield efficient deposition rates without causing thermal degradation of the compound. Another limitation of MLD stems from the fact that the reactivity of molecules with solid supports may be significantly reduced in the absence of solvent. Soft landing of mass-selected ions onto surfaces overcomes these major limitations of MLD. First, gentle ionization employing electrospray may produce ions of large thermally labile molecules that have very low volatility without inducing fragmentation or degradation. In addition, non-thermal ion sources may be used to generate a range of homogeneous or heterogeneous clusters and nanoparticles that are not susceptible to thermal volatilization. Moreover, ions may be accelerated prior to deposition to the kinetic energy necessary to overcome any potential barriers associated with interfacial reactions.

Soft landing of mass-selected ions is particularly well suited to the controlled immobilization of complex molecules, clusters, and nanoparticles on substrates. However, commercial-scale preparation of materials with this technique is limited due to the fact that the typical ion currents obtained with ESI are several orders of magnitude lower than those currently utilized in existing micro- and nanofabrication methods. The continued development of bright high transmission ESI sources[129-131], high power and fast repetition rate pulsed laser sources[25,132] and continuous sources based on DC and RF magnetron sputtering[43,65,133-135] is a crucial prerequisite for transitioning soft landing from a powerful tool in fundamental science to a practical approach for microfabrication. In the future, combining soft landing with ion mobility separation[113] will facilitate accurate control of both the primary and the secondary structure of complex ions, which is important both for practical applications as well as for investigating the effect of different surfaces on the secondary structure of immobilized ions. Furthermore, the unique capabilities of soft landing instrumentation will be used to manipulate molecules in the gas-phase, either through collisional fragmentation or ion-molecule reactions, to generate novel species that are not obtainable through synthesis in solution.

## Disclosures

The authors have nothing to disclose.

## Acknowledgements

This research was funded by the Office of Basic Energy Sciences, Division of Chemical Sciences, Geosciences & Biosciences of the U.S. Department of Energy (DOE). GEJ acknowledges support from the Linus Pauling Fellowship and the Laboratory Directed Research and Development Program at the Pacific Northwest National Laboratory (PNNL). This work was performed using EMSL, a national scientific user facility sponsored by the Department of Energy's Office of Biological and Environmental Research and located at PNNL. PNNL is operated by Battelle for the U.S. DOE.

## References

1. Gologan, B., Green, J. R., Alvarez, J., Laskin, J., & Cooks, R. G. Ion/surface reactions and ion soft-landing. *Physical Chemistry Chemical Physics.* **7**, 1490-1500 (2005).
2. Perez, A. *et al.* Functional nanostructures from clusters. *Int J Nanotechnol.* **7**, 523-574 (2010).
3. Laskin, J., Wang, P., & Hadjar, O. Soft-landing of peptide ions onto self-assembled monolayer surfaces: an overview. *Physical Chemistry Chemical Physics.* **10**, 1079-1090, doi:10.1039/b712710c|ISSN 1463-9076 (2008).
4. Cyriac, J., Pradeep, T., Kang, H., Souda, R., & Cooks, R. G. Low-Energy Ionic Collisions at Molecular Solids. *Chem Rev.* **112**, 5356-5411, doi: 10.1021/Cr200384k (2012).
5. Verbeck, G., Hoffmann, W., & Walton, B. Soft-landing preparative mass spectrometry. *Analyst.* **137**, 4393-4407 (2012).
6. Johnson, G. E., Hu, Q. C., & Laskin, J. Soft Landing of Complex Molecules on Surfaces. *Annu Rev Anal Chem.* **4**, 83-104, doi: 10.1146/annurev-anchem-061010-114028 (2011).
7. Ouyang, Z. *et al.* Preparing protein microarrays by soft-landing of mass-selected ions. *Science.* **301**, 1351-1354 (2003).

 

8. Blake, T. A. *et al.* Preparative linear ion trap mass spectrometer for separation and collection of purified proteins and peptides in arrays using ion soft landing. *Anal Chem.* **76**, 6293-6305, doi: 10.1021/Ac048981b (2004).
9. Blacken, G. R., Volny, M., Vaisar, T., Sadilek, M., & Turecek, F. *In situ* enrichment of phosphopeptides on MALDI plates functionalized by reactive landing of zirconium(IV)-n-propoxide ions. *Anal Chem.* **79**, 5449-5456, doi: 10.1021/Ac070790w (2007).
10. Blacken, G. R. *et al.* Reactive Landing of Gas-Phase Ions as a Tool for the Fabrication of Metal Oxide Surfaces for *In Situ* Phosphopeptide Enrichment. *J Am Soc Mass Spectr.* **20**, 915-926, doi:10.1016/j.jasms.2009.01.006 (2009).
11. Wang, P., & Laskin, J. Helical peptide arrays on self-assembled monolayer surfaces through soft and reactive landing of mass-selected ions. *Angew Chem Int Edit.* **47**, 6678-6680, doi: 10.1002/anie.200801366 (2008).
12. Hu, Q. C., Wang, P., & Laskin, J. Effect of the surface on the secondary structure of soft landed peptide ions. *Phys Chem Chem Phys.* **12**, 12802-12810, doi: 10.1039/C0cp00825g (2010).
13. Wang, P., Hadjar, O., & Laskin, J. Covalent immobilization of peptides on self-assembled monolayer surfaces using soft-landing of mass-selected ions. *J Am Chem Soc.* **129**, 8682-8683, doi:10.1021/ja071804i (2007).
14. Wang, P., Hadjar, O., Gassman, P. L., & Laskin, J. Reactive landing of peptide ions on self-assembled monolayer surfaces: an alternative approach for covalent immobilization of peptides on surfaces. *Physical Chemistry Chemical Physics.* **10**, 1512-1522, doi:10.1039/b717617a| ISSN 1463-9076 (2008).
15. Nanita, S. C., Takats, Z., Cooks, R. G., Myung, S., & Clemmer, D. E. Chiral enrichment of serine via formation, dissociation, and soft-landing of octameric cluster ions. *J Am Soc Mass Spectr.* **15**, 1360-1365, doi: 10.1016/j.jasms.2004.06.010 (2004).
16. Pepi, F. *et al.* Soft landed protein voltammetry. *Chem Commun* (33), 3494-3496, doi: 10.1039/B705668k (2007).
17. Mazzei, F. *et al.* Soft-landed protein voltammetry: A tool for redox protein characterization. *Anal Chem.* **80**, 5937-5944, doi:10.1021/ac8005389 (2008).
18. Mazzei, F., Favero, G., Frasconi, M., Tata, A., & Pepi, F. Electron-Transfer Kinetics of Microperoxidase-11 Covalently Immobilised onto the Surface of Multi-Walled Carbon Nanotubes by Reactive Landing of Mass-Selected Ions. *Chemistry-a European Journal.* **15**, 7359-7367, doi:10.1002/chem.200900887 (2009).
19. Rauschenbach, S. *et al.* Electrospray Ion Beam Deposition: Soft-Landing and Fragmentation of Functional Molecules at Solid Surfaces. *Acs Nano.* **3**, 2901-2910, doi:10.1021/nn900022p (2009).
20. Saf, R. *et al.* Thin organic films by atmospheric-pressure ion deposition. *Nat Mater.* **3**, 323-329, doi: 10.1038/Nmat1117 (2004).
21. Rader, H. J. *et al.* Processing of giant graphene molecules by soft-landing mass spectrometry. *Nature Materials.* **5**, 276-280 (2006).
22. Xirouchaki, C., & Palmer, R. E. Pinning and implantation of size-selected metal clusters: a topical review. *Vacuum.* **66**, 167-173, doi:Pii S0042-207x(01)00484-5 Doi 10.1016/S0042-207x(01)00484-5 (2002).
23. Xirouchaki, C., & Palmer, R. E. Deposition of size-selected metal clusters generated by magnetron sputtering and gas condensation: a progress review. *Philos T Roy Soc A.* **362**, 117-124 (2004).
24. Li, Z. Y. *et al.* Three-dimensional atomic-scale structure of size-selected gold nanoclusters. *Nature.* **451**, 46-U42, doi: 10.1038/Nature06470 (2008).
25. Heiz, U., Vanolli, F., Trento, L., & Schneider, W. D. Chemical reactivity of size-selected supported clusters: An experimental setup. *Rev Sci Instrum.* **68**, 1986-1994 (1997).
26. Heiz, U. *et al.* Chemical reactions on size-selected clusters on surfaces. *Nobel Symp.* **117**, 87-98 (2001).
27. Kunz, S. *et al.* Size-selected clusters as heterogeneous model catalysts under applied reaction conditions. *Phys Chem Chem Phys.* **12**, 10288-10291, doi: 10.1039/C0cp00288g (2010).
28. Wepasnick, K. A. *et al.* Surface Morphologies of Size-Selected Mo-100 +/- 2.5 and (MoO3)(67 +/- 1.5) Clusters Soft-Landed onto HOPG. *J Phys Chem C.* **115**, 12299-12307, doi: 10.1021/Jp202165u (2011).
29. Lim, D. C., Dietsche, R., Gantefor, G., & Kim, Y. D. Size-selected Au clusters deposited on SiO2/Si: Stability of clusters under ambient pressure and elevated temperatures. *Appl Surf Sci.* **256**, 1148-1151, doi: 10.1016/j.apsusc.2009.05.071 (2009).
30. Woodward, W. H., Blake, M. M., Luo, Z. X., Weiss, P. S., & Castleman, A. W. Soft-Landing Deposition of Al-17(-) on a Hydroxyl-Terminated Self-Assembled Monolayer. *J Phys Chem C.* **115**, 5373-5377, doi: 10.1021/Jp110527c (2011).
31. Benz, L. *et al.* Landing of size-selected Ag-n(+) clusters on single crystal $TiO_2$ (110)-(1x1) surfaces at room temperature. *J Chem Phys.* **122**, doi:Artn 081102 Doi 10.1063/1.1859271 (2005).
32. Tong, X. *et al.* Intact size-selected Au-n clusters on a $TiO_2$(110)-(1 x 1) surface at room temperature. *J Am Chem Soc.* **127**, 13516-13518, doi: 10.1021/Ja052778w (2005).
33. Kahle, S. *et al.* The Quantum Magnetism of Individual Manganese-12-Acetate Molecular Magnets Anchored at Surfaces. *Nano Lett.* **12**, 518-521, doi: 10.1021/Nl204141z (2012).
34. Proch, S., Wirth, M., White, H. S., & Anderson, S. L. Strong Effects of Cluster Size and Air Exposure on Oxygen Reduction and Carbon Oxidation Electrocatalysis by Size-Selected Pt-n (n <= 11) on Glassy Carbon Electrodes. *J Am Chem Soc.* **135**, 3073-3086, doi: 10.1021/Ja309868z (2013).
35. Kaden, W. E., Wu, T. P., Kunkel, W. A., & Anderson, S. L. Electronic Structure Controls Reactivity of Size-Selected Pd Clusters Adsorbed on $TiO_2$ Surfaces. *Science.* **326**, 826-829, doi:10.1126/science.1180297 (2009).
36. Binns, C. Nanoclusters deposited on surfaces. *Surf Sci Rep.* **44**, 1-49, doi: 10.1016/S0167-5729(01)00015-2 (2001).
37. Johnson, G. E., Priest, T., & Laskin, J. Coverage-Dependent Charge Reduction of Cationic Gold Clusters on Surfaces Prepared Using Soft Landing of Mass-Selected Ions. *J Phys Chem C.* **116**, 24977-24986, doi: 10.1021/Jp308795r (2012).
38. Johnson, G. E., Priest, T., & Laskin, J. Charge Retention by Gold Clusters on Surfaces Prepared Using Soft Landing of Mass Selected Ions. *Acs Nano.* **6**, 573-582, doi: 10.1021/Nn2039565 (2012).
39. Johnson, G. E., Wang, C., Priest, T., & Laskin, J. Monodisperse Au-11 Clusters Prepared by Soft Landing of Mass Selected Ions. *Anal Chem.* **83**, 8069-8072, doi: 10.1021/Ac202520p (2011).
40. Zachary, A. M., Bolotin, I. L., Asunskis, D. J., Wroble, A. T., & Hanley, L. Cluster Beam Deposition of Lead Sulfide Nanocrystals into Organic Matrices. *Acs Appl Mater Inter.* **1**, 1770-1777, doi: 10.1021/Am900301x (2009).
41. Ayesh, A. I., Qamhieh, N., Ghamlouche, H., Thaker, S., & El-Shaer, M. Fabrication of size-selected Pd nanoclusters using a magnetron plasma sputtering source. *J Appl Phys.* **107** (2010).
42. Ayesh, A. I., Thaker, S., Qamhieh, N., & Ghamlouche, H. Size-controlled Pd nanocluster grown by plasma gas-condensation method. *J Nanopart Res.* **13**, 1125-1131, doi: 10.1007/s11051-010-0104-2 (2011).
43. Ayesh, A. I., Qamhieh, N., Mahmoud, S. T., & Alawadhi, H. Fabrication of size-selected bimetallic nanoclusters using magnetron sputtering. *J Mater Res.* **27**, 2441-2446 (2012).


 

44. Datta, D., Bhattacharyya, S. R., Shyjumon, I., Ghose, D., & Hippler, R. Production and deposition of energetic metal nanocluster ions of silver on Si substrates. *Surf Coat Tech.* **203**, 2452-2457, doi: 10.1016/j.surfcoat.2009.02.114 (2009).
45. Majumdar, A. *et al.* Surface morphology and composition of films grown by size-selected Cu nanoclusters. *Vacuum.* **83**, 719-723 (2008).
46. Tang, J., Verrelli, E., & Tsoukalas, D. Assembly of charged nanoparticles using self-electrodynamic focusing. *Nanotechnology.* **20**, doi:Artn 365605 Doi 10.1088/0957-4484/20/36/365605 (2009).
47. Gracia-Pinilla, M. A., Martinez, E., Vidaurri, G. S., & Perez-Tijerina, E. Deposition of Size-Selected Cu Nanoparticles by Inert Gas Condensation. *Nanoscale Res Lett.* **5**, 180-188, doi: 10.1007/s11671-009-9462-z (2010).
48. Banerjee, A. N., Krishna, R., & Das, B. Size controlled deposition of Cu and Si nano-clusters by an ultra-high vacuum sputtering gas aggregation technique. *Appl Phys a-Mater.* **90**, 299-303, doi: 10.1007/s00339-007-4271-7 (2008).
49. Judai, K. *et al.* A soft-landing experiment on organometallic cluster ions: infrared spectroscopy of V(benzene)(2) in Ar matrix. *Chemical Physics Letters.* **334**, 277-284 (2001).
50. Mitsui, M., Nagaoka, S., Matsumoto, T., & Nakajima, A. Soft-landing isolation of vanadium-benzene sandwich clusters on a room-temperature substrate using n-alkanethiolate self-assembled monolayer matrixes. *J Phys Chem B.* **110**, 2968-2971 (2006).
51. Nagaoka, S., Matsumoto, T., Okada, E., Mitsui, M., & Nakajima, A. Room-temperature isolation of V(benzene)(2) sandwich clusters via soft-landing into n-alkanethiol self-assembled monolayers. *J Phys Chem B.* **110**, 16008-16017 (2006).
52. Nagaoka, S., Matsumoto, T., Ikemoto, K., Mitsui, M., & Nakajima, A. Soft-landing isolation of multidecker V-2(benzene)(3) complexes in an organic monolayer matrix: An infrared spectroscopy and thermal desorption study. *J Am Chem Soc.* **129**, 1528-1529 (2007).
53. Nagaoka, S., Ikemoto, K., Matsumoto, T., Mitsui, M., & Nakajima, A. Soft-landing isolation of gas-phase-synthesized transition metal-benzene complexes into a fluorinated self-assembled monolayer matrix. *J Phys Chem C.* **112**, 15824-15831, doi:10.1021/jp8055784 (2008).
54. Ikemoto, K., Nagaoka, S., Matsumoto, T., Mitsui, M., & Nakajima, A. Soft-Landing Experiments of Cr(benzene)(2) Sandwich Complexes onto a Carboxyl-Terminated Self-Assembled Monolayer Matrix. *J Phys Chem C.* **113**, 4476-4482, doi: 10.1021/Jp807137p (2009).
55. Nagaoka, S., Ikemoto, K., Horiuchi, K., & Nakajima, A. Soft- and Reactive-Landing of Cr(aniline)(2) Sandwich Complexes onto Self-Assembled Monolayers: Separation between Functional and Binding Sites. *J Am Chem Soc.* **133**, 18719-18727, doi: 10.1021/Ja205384q (2011).
56. Pepi, F. *et al.* Chemically Modified Multiwalled Carbon Nanotubes Electrodes with Ferrocene Derivatives through Reactive Landing. *J Phys Chem C.* **115**, 4863-4871, doi: 10.1021/Jp1100472 (2011).
57. Franchetti, V., Solka, B. H., Baitinger, W. E., Amy, J. W., & Cooks, R. G. Soft Landing of Ions as a Means of Surface Modification. *International Journal of Mass Spectrometry and Ion Processes.* **23**, 29-35 (1977).
58. Hadjar, O. *et al.* Design and performance of an instrument for soft landing of Biomolecular ions on surfaces. *Anal Chem.* **79**, 6566-6574, doi:10.1021/ac070600h|ISSN 0003-2700 (2007).
59. Peng, W. P. *et al.* Ion soft landing using a rectilinear ion trap mass spectrometer. *Anal Chem.* **80**, 6640-6649, doi:10.1021/ac800929w (2008).
60. Shen, J. W. *et al.* Soft landing of ions onto self-assembled hydrocarbon and fluorocarbon monolayer surfaces. *Int J Mass Spectrom.* **182**, 423-435, doi: 10.1016/S1387-3806(98)14251-3 (1999).
61. Bottcher, A., Weis, P., Bihlmeier, A., & Kappes, M. M. C-58 on HOPG: Soft-landing adsorption and thermal desorption. *Physical Chemistry Chemical Physics.* **6**, 5213-5217 (2004).
62. Klipp, B. *et al.* Deposition of mass-selected cluster ions using a pulsed arc cluster-ion source. *Appl Phys a-Mater.* **73**, 547-554 (2001).
63. Baker, S. H. *et al.* The construction of a gas aggregation source for the preparation of size-selected nanoscale transition metal clusters. *Rev Sci Instrum.* **71**, 3178-3183, doi:Pii [S0034-6748(00)01408-8] Doi 10.1063/1.1304868 (2000).
64. Haberland, H., Karrais, M., Mall, M., & Thurner, Y. Thin-Films from Energetic Cluster Impact - a Feasibility Study. *J Vac Sci Technol A.* **10**, 3266-3271, doi: 10.1116/1.577853 (1992).
65. Pratontep, S., Carroll, S. J., Xirouchaki, C., Streun, M., & Palmer, R. E. Size-selected cluster beam source based on radio frequency magnetron plasma sputtering and gas condensation. *Rev Sci Instrum.* **76** (2005).
66. Duncan, M. A. Invited Review Article: Laser vaporization cluster sources. *Rev Sci Instrum.* **83**, doi:Artn 041101 Doi 10.1063/1.3697599 (2012).
67. Wagner, R. L., Vann, W. D., & Castleman, A. W. A technique for efficiently generating bimetallic clusters. *Rev Sci Instrum.* **68**, 3010-3013, doi: 10.1063/1.1148058 (1997).
68. Harbich, W. *et al.* Deposition of Mass Selected Silver Clusters in Rare-Gas Matrices. *J Chem Phys.* **93**, 8535-8543, doi: 10.1063/1.459291 (1990).
69. Denault, J. W., Evans, C., Koch, K. J., & Cooks, R. G. Surface modification using a commercial triple quadrupole mass spectrometer. *Anal Chem.* **72**, 5798-5803 (2000).
70. Mayer, P. S. *et al.* Preparative separation of mixtures by mass spectrometry. *Anal Chem.* **77**, 4378-4384 (2005).
71. Badu-Tawiah, A. K., Wu, C. P., & Cooks, R. G. Ambient Ion Soft Landing. *Anal Chem.* **83**, 2648-2654, doi: 10.1021/Ac102940q (2011).
72. Badu-Tawiah, A. K., Campbell, D. I., & Cooks, R. G. Reactions of Microsolvated Organic Compounds at Ambient Surfaces: Droplet Velocity, Charge State, and Solvent Effects. *J Am Soc Mass Spectr.* **23**, 1077-1084, doi: 10.1007/s13361-012-0365-3 (2012).
73. Laskin, J., & Futrell, J. H. Activation of large ions in FT-ICR mass spectrometry. *Mass Spectrom Rev.* **24**, 135-167, doi: 10.1002/Mas.20012 (2005).
74. Laskin, J., & Futrell, J. H. Collisional activation of peptide ions in FT-ICR mass spectrometry. *Mass Spectrom Rev.* **22**, 158-181, doi: 10.1002/Mas.10041 (2003).
75. Wysocki, V. H., Joyce, K. E., Jones, C. M., & Beardsley, R. L. Surface-induced dissociation of small molecules, peptides,and non-covalent protein complexes. *J Am Soc Mass Spectr.* **19**, 190-208, doi: 10.1016/j.jasms.2007.11.005 (2008).
76. Abbet, S., Judai, K., Klinger, L., & Heiz, U. Synthesis of monodispersed model catalysts using softlanding cluster deposition. *Pure Appl Chem.* **74**, 1527-1535, doi: 10.1351/pac200274091527 (2002).
77. Molina, L. M. *et al.* Size-dependent selectivity and activity of silver nanoclusters in the partial oxidation of propylene to propylene oxide and acrolein: A joint experimental and theoretical study. *Catal Today.* **160**, 116-130, doi: 10.1016/j.cattod.2010.08.022 (2011).
78. Lei, Y. *et al.* Increased Silver Activity for Direct Propylene Epoxidation via Subnanometer Size Effects. *Science.* **328**, 224-228, doi: 10.1126/science.1185200 (2010).
79. Lee, S. *et al.* Selective Propene Epoxidation on Immobilized Au6-10 Clusters: The Effect of Hydrogen and Water on Activity and Selectivity. *Angew Chem Int Edit.* **48**, 1467-1471, doi: 10.1002/anie.200804154 (2009).
80. Peng, W. P. *et al.* Redox chemistry in thin layers of organometallic complexes prepared using ion soft landing. *Phys Chem Chem Phys.* **13**, 267-275, doi: 10.1039/C0cp01457e (2011).


 

81. Johnson, G. E., & Laskin, J. Preparation of Surface Organometallic Catalysts by Gas-Phase Ligand Stripping and Reactive Landing of Mass-Selected Ions. *Chem-Eur J.* **16**, 14433-14438, doi: 10.1002/chem.201002292 (2010).
82. Castleman, A. W., & Jena, P. Clusters: A bridge between disciplines. *P Natl Acad Sci USA.* **103**, 10552-10553, doi: 10.1073/pnas.0601783103 (2006).
83. Jena, P., & Castleman, A. W. Clusters: A bridge across the disciplines of physics and chemistry. *P Natl Acad Sci USA.* **103**, 10560-10569, doi: 10.1073/pnas.0601782103 (2006).
84. Castleman, A. W., & Jena, P. Clusters: A bridge across the disciplines of environment, materials science, and biology. *P Natl Acad Sci USA.* **103**, 10554-10559, doi: 10.1073/pnas.0601780103 (2006).
85. Yoon, B. *et al.* Charging effects on bonding and catalyzed oxidation of CO on Au-8 clusters on MgO. *Science.* **307**, 403-407, doi: 10.1126/science.1104168 (2005).
86. Landman, U., Yoon, B., Zhang, C., Heiz, U., & Arenz, M. Factors in gold nanocatalysis: oxidation of CO in the non-scalable size regime. *Top Catal.* **44**, 145-158, doi: 10.1007/s11244-007-0288-6 (2007).
87. Habibpour, V. *et al.* Novel Powder-Supported Size-Selected Clusters for Heterogeneous Catalysis under Realistic Reaction Conditions. *J Phys Chem C.* **116**, 26295-26299, doi: 10.1021/Jp306263f (2012).
88. Herzing, A. A., Kiely, C. J., Carley, A. F., Landon, P., & Hutchings, G. J. Identification of active gold nanoclusters on iron oxide supports for CO oxidation. *Science.* **321**, 1331-1335, doi: 10.1126/science.1159639 (2008).
89. Turner, M. *et al.* Selective oxidation with dioxygen by gold nanoparticle catalysts derived from 55-atom clusters. *Nature.* **454**, 981-U931, doi: 10.1038/Nature07194 (2008).
90. Yin, F., Xirouchaki, C., Guo, Q. M., & Palmer, R. E. High-temperature stability of size-selected gold nanoclusters pinned on graphite. *Adv Mater.* **17**, 731-734, doi: 10.1002/adma.200401095 (2005).
91. Palomba, S., & Palmer, R. E. Patterned films of size-selected Au clusters on optical substrates. *J Appl Phys.* **101**, doi:Artn 044304 Doi 10.1063/1.2512480 (2007).
92. Yin, F., Lee, S. S., Abdela, A., Vajda, S., & Palmer, R. E. Communication: Suppression of sintering of size-selected Pd clusters under realistic reaction conditions for catalysis. *J Chem Phys.* **134**, doi:Artn 141101 Doi 10.1063/1.3575195 (2011).
93. Zamboulis, A., Moitra, N., Moreau, J. J. E., Cattoen, X., & Man, M. W. C. Hybrid materials: versatile matrices for supporting homogeneous catalysts. *J Mater Chem.* **20**, 9322-9338, doi: 10.1039/C000334d (2010).
94. Notestein, J. M., & Katz, A. Enhancing heterogeneous catalysis through cooperative hybrid organic-inorganic interfaces. *Chem-Eur J.* **12**, 3954-3965, doi: 10.1002/chem.200501152 (2006).
95. Love, J. C., Estroff, L. A., Kriebel, J. K., Nuzzo, R. G., & Whitesides, G. M. Self-assembled monolayers of thiolates on metals as a form of nanotechnology. *Chem Rev.* **105**, 1103-1169, doi: 10.1021/Cr0300789 (2005).
96. Peng, W. P., Goodwin, M. P., Chen, H., Cooks, R. G., & Wilker, J. Thermal formation of mixed-metal inorganic complexes at atmospheric pressure. *Rapid Commun Mass Sp.* **22**, 3540-3548, doi: 10.1002/Rcm.3763 (2008).
97. Alvarez, J. *et al.* Preparation and *in situ* characterization of surfaces using soft landing in a Fourier transform ion cyclotron resonance mass spectrometer. *Anal Chem.* **77**, 3452-3460 (2005).
98. Cyriac, J., Li, G. T., & Cooks, R. G. Vibrational Spectroscopy and Mass Spectrometry for Characterization of Soft Landed Polyatomic Molecules. *Anal Chem.* **83**, 5114-5121, doi: 10.1021/Ac200118f (2011).
99. Johnson, G. E., Lysonski, M., & Laskin, J. *In Situ* Reactivity and TOF-SIMS Analysis of Surfaces Prepared by Soft and Reactive Landing of Mass-Selected Ions. *Anal Chem.* **82**, 5718-5727, doi:10.1021/ac100734g (2010).
100. Nie, Z. X. *et al. In Situ* SIMS Analysis and Reactions of Surfaces Prepared by Soft Landing of Mass-Selected Cations and Anions Using an Ion Trap Mass Spectrometer. *J Am Soc Mass Spectr.* **20**, 949-956, doi:10.1016/j.jasms.2009.02.019 (2009).
101. Gologan, B. *et al.* Ion soft-landing into liquids: Protein identification, separation, and purification with retention of biological activity. *J Am Soc Mass Spectr.* **15**, 1874-1884 (2004).
102. Judai, K., Abbet, S., Worz, A. S., Rottgen, M. A., & Heiz, U. Turn-over frequencies of catalytic reactions on nanocatalysts measured by pulsed molecular beams and quantitative mass spectrometry. *Int J Mass Spectrom.* **229**, 99-106, doi: 10.1016/S1387-3806(03)00261-6 (2003).
103. Cyriac, J., Wleklinski, M., Li, G. T., Gao, L., & Cooks, R. G. *In situ* Raman spectroscopy of surfaces modified by ion soft landing. *Analyst.* **137**, 1363-1369, doi: 10.1039/C2an16163j (2012).
104. Hu, Q. C., Wang, P., Gassman, P. L., & Laskin, J. *In situ* Studies of Soft- and Reactive Landing of Mass-Selected Ions Using Infrared Reflection Absorption Spectroscopy. *Anal Chem.* **81**, 7302-7308, doi:10.1021/ac901149s (2009).
105. Volny, M. *et al.* Surface-enhanced Raman spectroscopy of soft-landed polyatomic ions and molecules. *Anal Chem.* **79**, 4543-4551 (2007).
106. Kartouzian, A. *et al.* Cavity ring-down spectrometer for measuring the optical response of supported size-selected clusters and surface defects in ultrahigh vacuum. *J Appl Phys.* **104** (2008).
107. Kaden, W. E., Kunkel, W. A., Roberts, F. S., Kane, M., & Anderson, S. L. CO adsorption and desorption on size-selected Pdn/$TiO_2$(110) model catalysts: Size dependence of binding sites and energies, and support-mediated adsorption. *J Chem Phys.* **136**, doi:Artn 204705 Doi 10.1063/1.4721625 (2012).
108. Price, S. P. *et al.* STM characterization of size-selected V-1, V-2, VO and VO2 clusters on a $TiO_2$ (110)-(1 x 1) surface at room temperature. *Surf Sci.* **605**, 972-976, doi: 10.1016/j.susc.2011.02.016 (2011).
109. Benz, L. *et al.* Pinning mononuclear Au on the surface of titania. *J Phys Chem B.* **110**, 663-666, doi: 10.1021/Jp0559635 (2006).
110. Deng, Z. T. *et al.* A Close Look at Proteins: Submolecular Resolution of Two- and Three-Dimensionally Folded Cytochrome c at Surfaces. *Nano Lett.* **12**, 2452-2458, doi: 10.1021/Nl3005385 (2012).
111. Di Vece, M., Palomba, S., & Palmer, R. E. Pinning of size-selected gold and nickel nanoclusters on graphite. *Phys Rev B.* **72**, doi:Artn 073407 Doi 10.1103/Physrevb.72.073407 (2005).
112. Benesch, J. L. P. *et al.* Separating and visualisiing protein assemblies by means of preparative mass spectrometry and microscopy. *J Struct Biol.* **172**, 161-168, doi: 10.1016/j.jsb.2010.03.004 (2010).
113. Davila, S. J., Birdwell, D. O., & Verbeck, G. F. Drift tube soft-landing for the production and characterization of materials: Applied to Cu clusters. *Rev Sci Instrum.* **81**, doi:034104 10.1063/1.3361041 (2010).
114. Rauschenbach, S. *et al.* Electrospray ion beam deposition of clusters and biomolecules. *Small.* **2**, 540-547 (2006).
115. Hadjar, O., Futrell, J. H., & Laskin, J. First observation of charge reduction and desorption kinetics of multiply protonated peptides soft landed onto self-assembled monolayer surfaces. *J Phys Chem C.* **111**, 18220-18225, doi: 10.1021/Jp075293y (2007).
116. Hadjar, O., Wang, P., Futrell, J. H., & Laskin, J. Effect of the Surface on Charge Reduction and Desorption Kinetics of Soft Landed Peptide Ions. *J Am Soc Mass Spectr.* **20**, 901-906, doi:10.1016/j.jasms.2008.12.025 (2009).


 

117. Heiz, U., & Bullock, E. L. Fundamental aspects of catalysis on supported metal clusters. *J Mater Chem.* **14**, 564-577, doi: 10.1039/B313560h (2004).
118. Nogues, C., & Wanunu, M. A rapid approach to reproducible, atomically flat gold films on mica. *Surf Sci.* **573**, L383-L389, doi: 10.1016/j.susc.2004.10.019 (2004).
119. Kawasaki, M., & Uchiki, H. Sputter deposition of atomically flat Au(111) and Ag(111) films. *Surf Sci.* **388**, L1121-L1125 (1997).
120. Laskin, J., Denisov, E. V., Shukla, A. K., Barlow, S. E., & Futrell, J. H. Surface-induced dissociation in a Fourier transform ion cyclotron resonance mass spectrometer: Instrument design and evaluation. *Anal Chem.* **74**, 3255-3261, doi:Unsp Ac025514q Doi 10.1021/Ac025514q (2002).
121. Mize, T. H. *et al.* A modular data and control system to improve sensitivity, selectivity, speed of analysis, ease of use, and transient duration in an external source FTICR-MS. *Int J Mass Spectrom.* **235**, 243-253, doi: 10.1016/j.ijms.2004.05.003 (2004).
122. Mallick, P. K., Danzer, G. D., Strommen, D. P., & Kincaid, J. R. Vibrational-Spectra and Normal-Coordinate Analysis of Tris(Bipyridine)Ruthenium(Ii). *J Phys Chem-Us.* **92**, 5628-5634, doi: 10.1021/J100331a018 (1988).
123. Strommen, D. P., Mallick, P. K., Danzer, G. D., Lumpkin, R. S., & Kincaid, J. R. Normal-Coordinate Analyses of the Ground and 3mlct Excited-States of Tris(Bipyridine)Ruthenium(Ii). *J Phys Chem-Us.* **94**, 1357-1366, doi: 10.1021/J100367a031 (1990).
124. Kim, H., Lee, H. B. R., & Maeng, W. J. Applications of atomic layer deposition to nanofabrication and emerging nanodevices. *Thin Solid Films.* **517**, 2563-2580 (2009).
125. Du, Y., & George, S. M. Molecular layer deposition of nylon 66 films examined using *in situ* FTIR spectroscopy. *J Phys Chem C.* **111**, 8509-8517 (2007).
126. Yoshimura, T., Tatsuura, S., & Sotoyama, W. Polymer-Films Formed with Monolayer Growth Steps by Molecular Layer Deposition. *Appl Phys Lett.* **59**, 482-484 (1991).
127. Loscutoff, P. W., Zhou, H., Clendenning, S. B., & Bent, S. F. Formation of Organic Nanoscale Laminates and Blends by Molecular Layer Deposition. *Acs Nano.* **4**, 331-341 (2010).
128. George, S. M., Yoon, B., & Dameron, A. A. Surface Chemistry for Molecular Layer Deposition of Organic and Hybrid Organic-Inorganic Polymers. *Accounts Chem Res.* **42**, 498-508 (2009).
129. Marginean, I., Page, J. S., Tolmachev, A. V., Tang, K. Q., & Smith, R. D. Achieving 50% Ionization Efficiency in Subambient Pressure Ionization with Nanoelectrospray. *Anal Chem.* **82**, 9344-9349 (2010).
130. Page, J. S., Tang, K., Kelly, R. T., & Smith, R. D. Subambient pressure ionization with nanoelectrospray source and interface for improved sensitivity in mass spectrometry. *Anal Chem.* **80**, 1800-1805 (2008).
131. Kelly, R. T., Page, J. S., Tang, K. Q., & Smith, R. D. Array of chemically etched fused-silica emitters for improving the sensitivity and quantitation of electrospray ionization mass spectrometry. *Anal Chem.* **79**, 4192-4198 (2007).
132. Spraggins, J. M., & Caprioli, R. High-Speed MALDI-TOF Imaging Mass Spectrometry: Rapid Ion Image Acquisition and Considerations for Next Generation Instrumentation. *J Am Soc Mass Spectr.* **22**, 1022-1031 (2011).
133. Majumdar, A. *et al.* Development of metal nanocluster ion source based on dc magnetron plasma sputtering at room temperature. *Rev Sci Instrum.* **80** (2009).
134. Ganeva, M., Pipa, A. V., & Hippler, R. The influence of target erosion on the mass spectra of clusters formed in the planar DC magnetron sputtering source. *Surf Coat Tech.* **213**, 41-47 (2012).
135. Tang, J., Verrelli, E., & Tsoukalas, D. Selective deposition of charged nanoparticles by self-electric focusing effect. *Microelectron Eng.* **86**, 898-901 (2009).


 